Economic nonlinear model predictive control of fatigue for a hybrid wind-battery generation system

Abhinav Anand[1], Stefan Loew[1], and Carlo L. Bottasso[1]

[1]Technical University of Munich, Wind Energy Institute, Boltzmannstrasse 15, 85748 Garching bei Muenchen, Germany.

E-mail: abhinav.anand@tum.de

Abstract. An economic nonlinear model predictive controller (ENMPC) is formulated for a wind turbine-battery hybrid generation system. The controller aims to maximize the operational profit of the generator by balancing between generated wind power and turbine tower fatigue as well as battery cyclic fatigue. Other than the tower fore-aft fatigue, tower side-side fatigue is also considered to assess impact on overall economic performance. A moving horizon estimator (MHE) is formulated to provide meaningful initialization to the ENMPC in presence of plant model mismatch.The formulated controller utilizes the parametric online rainflow counting (PORFC) approach for direct cyclic fatigue cost minimization within ENMPC. The closed-loop simulation shows significantly higher profit compared to a realistic base-case scenario and relatively higher profit compared to another economic controller.

1. Introduction

Large scale grid integration of wind power has the potential to drive the transition towards a cleaner energy system. However, wind power is inherently characterized by generation variability and uncertainty. One emerging approach involves hybridizing the wind energy systems with energy storage systems such as batteries. Conventionally, such a hybrid generation system aims to maximize the wind power capture while using battery to compensate for uncertainty and variability of generated wind power, abiding to the grid requirements at the same time. However, operating such a system in closed loop with an economically optimal controller can allow profit-optimal operation, by balancing between the generated revenues and system costs (such as fatigue damage of components or other operational expenses). Fatigue damage corresponds to damage of an energy unit during its operation phase and results in reduction of overall operational life of the unit. For a wind turbine, damage refers to the structural fatigue in the turbine components such as tower, blades, drive-train, and others. Out of these, tower fatigue damage is of critical importance, as it not only serves as a crucial design driver but also has significant impact on operational expenses of the turbine [1, 2]. For a battery storage unit, fatigue damage corresponds to the permanent capacity loss due to application of charging and discharging cycles [3]. These damages result in significant economic cost to the plant owner.

A dynamic economic optimization of wind and battery based hybrid system is seldom witnessed in the literature. In [4] and [5], only the battery damage is considered within an optimal control framework, where the damage evaluation approach is simplified and a simultaneous optimization of damage cost and revenue for accurate economic evaluation is missing. In [6], an MPC based supervisory controller has been formulated which, while

maximizing the dispatchable power of the hybrid system, focuses on damping the turbine shaft twist to alleviate shaft fatigue and reducing the battery charge throughput to minimize battery cyclic capacity loss. However, the MPC utilizes a simplified wind turbine model consisting only of the generator degree of freedom and an overly simplified battery model representing only the state of charge dynamics. To the best of our knowledge, for a hybrid generation system, a direct and accurate minimization of wind turbine and battery cyclic fatigue damage and their simultaneous economic balancing against revenue within optimal control framework is presented for the first time in our previous work [7]. However, in [7], a low-fidelity wind turbine model with only six states is considered. Also, tower fatigue damage evaluation includes only tower fore-aft oscillations. In that work, no consideration is given to the tower side-side dynamics as the reduced fore-aft oscillation might appear as increased side-side oscillations. Moreover, perfect measurement of all the hybrid system model states, including tower tip fore-aft displacement and velocity, is assumed.

The objective of this work is to extend the simplified formulation presented in [7] towards a more complex and realistic setup. The novelty of this work lies in formulating the economic nonlinear MPC (ENMPC) for a hybrid generation system comprising of high-fidelity wind turbine and battery models. The impact of plant model mismatch on closed-loop controller performance is assessed and addressed, as the controller utilizes a reduced order model with fewer degrees of freedom than the plant model. A moving horizon estimator (MHE) is additionally formulated to provide initial value estimates to ENMPC for the internal model states that could not be directly measured on a real plant. The closed-loop formulation is extended to take into consideration not just tower fore-aft dynamics but also tower side-side dynamics. This is to evaluate the impact of optimal control actions on side-side dynamics and contribution of side-side dynamics on overall closed-loop economic performance. Furthermore, the performance of the formulated economic controller is evaluated against a realistic base-case scenario and another standard controller employing state-of-the-art indirect fatigue minimization strategy.

2. Cyclic fatigue damage minimization in MPC framework

An accurate evaluation of fatigue within the MPC framework is imperative for optimal economic balancing. The Rainflow counting (RFC) algorithm is the most widely used approach for evaluating fatigue damage [8]. This includes identifying the reversals (extrema) in the given cyclic stress trajectory, to obtain the number of cycles and corresponding cycle characteristics, such as cycle mean, weight, and amplitude. A detailed account of calculating cyclic damage for wind turbine tower root stress and for battery is presented in [7, 9, 10]. The standard RFC approach calculates, for given stress samples $\boldsymbol{\sigma}(k)$, the total damage due to both half- and full-cycles, and then discards all the stress samples [11]. *Residue* refers to those stress samples that have resulted in a half(open)-cycle and are thus not part of a full(closed)-cycle yet [11]. Understanding the impact of *Residue* stress samples $\boldsymbol{\sigma}_{residue}(k)$ on the resulting cyclic damage is of the utmost importance as these samples, in future, have the possibility to form an open cycle with higher cycle amplitude having higher cyclic damage. As a consequence, an improper consideration of stress history can lead to the under-evaluation of the resulting cyclic fatigue damage. To this extent, a one step time discrete RFC algorithm, explained in detail in [10], is utilized, where residue samples from the past are stored and merged with incoming stress sample prior to Rainflow analysis. The impact of residue in improving closed-loop economic performance has also been shown in [7], where a stress history-aware controller performs better than a blinded controller (unaware of the stress history).

The standard cyclic fatigue evaluation using the RFC algorithm can not be directly used for cyclic fatigue minimization within the MPC framework. This is because the implementation of RFC contains algorithmic branches and loops which results in discontinuous output behavior. As a result, the calculation of sensitivities required for numerical optimization is not possible. An

example implementation in MATLAB has been analyzed in [9], where the inherent algorithmic loops have been highlighted clearly. Moreover, as cyclic damage is a long term effect [9], this requires storing and properly accounting for the impact of stress histories within the MPC framework.

The aforementioned challenges of direct implementation of RFC in MPC are overcome by utilizing the concept of Parameteric Online RFC (PORFC). This includes externalizing the damage evaluation step from the MPC optimization step by performing an online Rainflow analysis based on a stress history (*Residue*) to generate time-varying parameters. Here, all the discontinuous parts of the cyclic damage estimation procedure are performed in a pre-processing step before each execution of the MPC optimization step. In order to have the externalized cyclic fatigue evaluation on the same stress profile as MPC, the pre-processing step has to start with a predictive forward simulation using the controller internal model

$$\dot{\mathbf{x}}(t) = \mathbf{F}_h(\mathbf{x}(t), \mathbf{u}(t), \mathbf{d}(t)), \tag{1}$$

with the same sampling time T_{ctrl}, and horizon length $T_{horizon}$ as MPC. Here, $\mathbf{x}(t)$, $\mathbf{u}(t)$, and $\mathbf{d}(t)$ represent continuous system states, control variables, and external disturbance respectively, and function $\mathbf{F}_h(.)$ represents the mapping of ordinary differential equations governing the continuous dynamics of the system. The PORFC concept has been explained in detail in our previous work [10]. The output of the pre-processing PORFC approach is the time-varying cycle mean $\sigma^{\mathrm{PORFC}}_{\mathrm{m,c1/2}}$ and cycle weight parameters $\sigma^{\mathrm{PORFC}}_{\mathrm{w,c1/2}}$:

$$\mathbf{p}^{PORFC} = \left(\sigma^{\mathrm{PORFC}}_{\mathrm{m,c1}}, \sigma^{\mathrm{PORFC}}_{\mathrm{m,c2}}, \sigma^{\mathrm{PORFC}}_{\mathrm{w,c1}}, \sigma^{\mathrm{PORFC}}_{\mathrm{w,c2}}\right), \tag{2}$$

which is defined as a piece-wise constant function over the control intervals of the prediction horizon. Although a stress sample is not allocated uniquely to one identified cycle, it can at maximum be part of two cycles [12]. Hence, the Rainflow algorithm provides one or two mean stress values per extremum. These mean stress values are considered as optimization- or tracking-goals for the current MPC-step.

In the objective function of the MPC, the PORFC parameters $\mathbf{p}^{PORFC}$ are used to time-continuously calculate the cyclic damage over the horizon and accumulate it via integration. Consequently, the cyclic damage term of PORFC is defined by a time-integral over two cost terms, where each represents one potential cycle-contribution of a stress sample [10]. The rate of cyclic damage

$$\dot{D}^{PORFC}_{cyc}(t) = \frac{\mathrm{d}\Delta D^{PORFC}_{cyc}\left(\sigma(t), \mathbf{p}^{PORFC}(t)\right)}{\mathrm{d}t} = \frac{1}{T_{ctrl}} \sum_{c=1}^{2} D^{\mathrm{PORFC}}_{cyc,c}\left(\sigma(t), \sigma^{\mathrm{PORFC}}_{m,c}(t), \sigma^{\mathrm{PORFC}}_{w,c}(t)\right) \quad . \tag{3}$$

can thus be used to formulate cyclic damage minimization objectives for the optimal control problem.

3. Optimal control problem formulation

An ENMPC utilizes an internal model of the plant (refer to Eq. (1)) to predict the system states over a future horizon. These predictions are used to calculate economically optimal control variables by optimizing a chosen realistic and meaningful economic objective function (maximizing profit by balancing between revenue and costs). The optimization problem, in addition to the system state and input constraints, should also ensure that the total generation of

the hybrid plant matches a reference power, which is particularly essential in tracking the varying power demanded by the electricity grid. Since the controller internal model has fewer degrees of freedom compared to the plant model, not all relevant system dynamics is captured using the internal model, resulting in incorrect economic objective values within the MPC optimization. The controller internal model is initialized using the currently measured states $\widetilde{\mathbf{x}}$ as initial states $\mathbf{x}_0$. However, not all system states of the controller internal model of the wind turbine can actually be measured directly on a real plant. As a consequence, a Moving Horizon Estimator (MHE) is additionally formulated to provide initial value estimates $\mathbf{x}_{est}$ to the ENMPC internal model, using the available measurements $\widetilde{\mathbf{x}}$ from the high-fidelity plant model.

3.1. Controller-internal model description

3.1.1. Wind turbine dynamics A reduced order model of the NREL 5 MW wind turbine has been considered in this work. This section summarizes the modeling approach which has been presented in detail in [13]. The incident wind V_w induces an aerodynamic torque T_Q in the rotor shaft and a thrust force F_T on the rotor. The aerodynamic torque directly couples with the drive-train dynamics

$$J_r\dot{\omega} = T_Q - T_g, \tag{4}$$

where J_r, ω, and T_g represent the rotor moment of inertia, rotor angular velocity, and generator torque referred to the rotor shaft side, respectively. The aerodynamic thrust force F_T coupled with the drive-train dynamics excite oscillations in the tower. These can be quantified by using the tower tip deflection in the horizontal (fore-aft) direction $d_{T_{FA}}$, having dynamics

$$\ddot{d}_{T_{FA}} = \frac{1}{a_1}(F_{T_{FA}} - a_2\dot{d}_{T_{FA}} - a_3 d_{T_{FA}}), \tag{5}$$

resulting in cyclic stresses $\sigma(t)_{FA}$ at the tower root. Here, $F_{T_{FA}}$ represents the horizontal component of the impinging thrust force F_T. The turbine model has two control variables: the rate of change of the generator torque $\dot{T}_g$ and the blade pitch actuator set-point β_c with blade dynamics

$$\ddot{\beta}_b = -a_4\dot{\beta}_b - a_5(\beta_b - \beta_c). \tag{6}$$

Here, β_b represents the collective blade pitch angle and the parameters a_1 through a_5 are fixed model parameters representing turbine properties [13]. Non-linearity in the model originates from $T_Q(\omega, \beta_b, (V_w - \dot{d}_{T_{FA}}))$ and $F_{T_{FA}}(\omega, \beta_b, (V_w - \dot{d}_{T_{FA}}))$, which are computed offline at stationary operating points using the *OpenFAST* wind turbine simulator.

3.1.2. Battery dynamics An electrical equivalent circuit model of a 1MW/1MWh Li-ion battery has been considered in this work. This section summarizes the modeling approach which is presented in detail in [10]. The battery model consists of three sub-models: electrical, thermal, and degradation. For a given control variable P_B, denoting battery power, the electrical sub-model captures the battery current $I(t)$ dynamics and the state of charge $SOC(t)$ dynamics

$$\dot{SOC} = -\frac{I}{Q}. \tag{7}$$

Here, Q represents the maximum charge capacity of the battery at a given time. Q always decreases over time and usage because of the permanent loss in the capacity of the battery over time (calendric damage Q_{cal}), calculated using

$$\dot{Q}_{cal} = f_1(SOC) f_2(T)\sqrt{t}. \tag{8}$$

Furthermore, it also decreases over charging and discharging operations (cyclic damage Q_{cyc}), calculated by applying the one-step time discrete RFC algorithm (refer to Sect. 2) over SOC samples. The functions $f_1(SOC)$ and $f_2(T)$ denote the dependency of the state of charge SOC and battery temperature T on the calendric capacity loss. The battery thermal model captures the evolution of battery temperature $T(t)$ dynamics

$$\dot{T} = \frac{1}{C_H}(I^2 R_{int} - C_R(T - T_{ambient})), \tag{9}$$

based on a lumped heat capacitance model [14], where C_R and C_H denote cooling rate and heat capacity respectively. Here, $T_{ambient}$ denotes the ambient temperature which is considered to be fixed at 298.15 K.

3.1.3. Hybrid system model The reduced-order wind turbine and battery based hybrid system model, as shown in Eq. (1), consists of ten system states $\mathbf{x} = (\mathbf{x_{WT}}, \mathbf{x_B})$ and three control input variables $\mathbf{u} = (\beta_c, \dot{T}_g, P_B)$. Out of these, six states correspond to the wind turbine dynamics $\mathbf{x_{WT}} = (\omega, d_{T_{FA}}, \dot{d}_{T_{FA}}, \beta_b, \dot{\beta}_b, T_g)$, and four states denote the battery dynamics $\mathbf{x_B} = (T, SOC, Q_{cal}, Q_{cyc})$. The wind speed V_w is considered as a disturbance input to the model $\mathbf{d} = (V_w)$. In the present work, the turbine is assumed to receive perfect foresight of the incoming rotor-equivalent wind speed from a Light Detection and Ranging (LiDAR) sensor.

3.2. Plant model
The 5MW NREL *OpenFAST* wind turbine simulator is utilized in this work as the plant model. The *OpenFAST* simulator (including pitch and torque actuators but excluding yaw mechanism), contains 33 system states (8 tower states, 6 states for each of the three blades, 2 states for drive-shaft torsion, 2 states for rotor rotation, 2 states for collective blade pitch actuation, and 1 state for generator torque actuation) [15]. On the contrary, the ENMPC internal model consists only of 6 wind turbine specific states (refer to Sect. 3.1). Moreover, some of the states of the internal model can not be measured directly on a real plant. For example, the tower tip deflection $d_{T_{FA}}$ and velocity $\dot{d}_{T_{FA}}$ for fore-aft oscillations can not be measured on a real turbine using standard sensors.

The battery plant model is similar to the battery internal model without few modeling approximations (refer to [7] and [10] for details).

3.3. MPC optimization problem
The economic optimization problem is formulated as

$$\min_{\mathbf{u},\mathbf{s}} -(J^{WT}_{generation})^2 + (J^{WT}_{towerfatigue})^2 + (J^{B}_{cyclicloss})^2 \quad + \quad \int_{t_0}^{t_{end}} (10^3 s_1^2 \quad + \quad 10^6 s_2^2)\mathrm{dt} \tag{10a}$$

subject to

$$\dot{\mathbf{x}} = \mathbf{F}_h(\mathbf{x}, \mathbf{u}, \mathbf{d}) \tag{10b}$$

$$\underline{\mathbf{x}_{aug}} \leq \mathbf{x}_{aug} \leq \overline{\mathbf{x}_{aug}} \tag{10c}$$

$$\underline{\mathbf{u}} \leq \mathbf{u} \leq \overline{\mathbf{u}} \tag{10d}$$

$$\underline{\mathbf{s}} \leq \mathbf{s} \leq \overline{\mathbf{s}} \tag{10e}$$

$$\eta_{gen}\omega T_g + P_B + s_2 = P_{demand}^{grid}. \tag{10f}$$

The problem is solved in an online MPC fashion for the hybrid system model described in Sect. 3.1. Here the interval $t \in [t_0, t_{end}]$ denotes the prediction horizon $T_{horizon}$ of MPC. The optimization variables are the control variables $\mathbf{u} = (\beta_b, \dot{T}_g, P_B)$ and the slack variables $\mathbf{s} = (s_1, s_2)$.

The purpose of introducing slack variables is to achieve recursive feasibility of the MPC optimization problem in the presence of model uncertainties and system perturbations [16]. In the present formulation, the state variable ω and the wind turbine electrical power output ωT_g are augmented using the bounded slack variables s_1 and s_2, respectively, as suggested in [16]. The augmented system states $\mathbf{x}_{aug}$ can be represented as $\mathbf{x}_{aug} = (\omega + s_1, d_{T_{FA}}, \dot{d}_{T_{FA}}, \beta_b, \dot{\beta}_b, T_g, T, SOC)$.

The optimization objective aims to maximize the generated profit and has the components described in the following.

Maximizing wind power generation: The wind power generation is maximized by considering the aerodynamic power capture

$$J_{generation}^{WT} = w_P \int_{t_0}^{t_{end}} (\omega(t) T_Q(\omega, \beta_b, (V_w - \dot{d}_{T_{FA}})))\mathrm{dt}, \tag{11}$$

where w_P denotes the revenue rate for providing electricity to the grid. It should be noted that even though the revenue is accrued based on the overall electrical power generation, in this work the aerodynamic power is maximized. This is to avoid the greedy extraction of rotor kinetic energy by MPC (referred to as *turnpike effect* in [16]).

Minimizing wind turbine tower fatigue: The tower cyclic fatigue damage $J_{towerfatigue}^{WT}$, because of tower root fore-aft cyclic stress σ_{FA}, is minimized by a direct penalization of fatigue cost using a continuous estimation of fatigue cost rate via the PORFC approach (refer to Eq. 3 and for details check [9])

$$J_{towerfatigue}^{WT} = \int_{t_0}^{t_{end}} (J_{cyc,\sigma_{FA}}^{PORFC})\mathrm{dt},$$

$$J_{cyc,\sigma_{FA}}^{PORFC} = \frac{1}{T_{ctrl}} \sum_{c=1}^{2} J_{cyc,c,\sigma_{FA}}^{\mathrm{PORFC}}(\sigma_{FA}(t), \sigma_{FA_{m,c}}^{\mathrm{PORFC}}(t), \sigma_{FA_{w,c}}^{\mathrm{PORFC}}(t)). \tag{12}$$

In addition to the direct fatigue penalization approach, an indirect fatigue penalization approach using tower-tip velocity (TTVP) has also been formulated as a reference

$$J_{towerfatigue}^{WT} = w_{fatigue}^{TTVP} \int_{t_0}^{t_{end}} \frac{1}{2T_{horizon} P_{g,max}^{WT}} m_T (\dot{d}_{T_{FA}})^2 \mathrm{dt}, \tag{13}$$

to evaluate the performance of PORFC for accurate tower fatigue minimization inside the MPC framework. Here, the TTVP approach has been implemented as a quadratic penalization of kinetic energy of lumped tower mass m_T given as $m_T(\dot{d}_{T_{FA}})^2$, averaged over the MPC prediction horizon $T_{horizon}$. An additional division by the wind turbine rated power $P_{g,max}^{WT}$ is used for scaling, which is beneficial for optimization. The use of indirect fatigue penalization is quite common in the literature [17, 18], where a damage-related value rather than the actual damage is penalized. Consequently, the penalization weight term $w_{fatigue}^{TTVP}$ has to be carefully chosen, as the indirect fatigue term has different units than revenue generated due to harvested energy.

Minimizing battery cyclic fatigue: The battery cyclic fatigue damage $J^B_{cyclicloss}$ is minimized by a direct penalization of fatigue cost using a continuous estimation of fatigue cost rate via the PORFC approach (refer to Eq. (3) and for details check [9])

$$J^B_{cyclicloss} = w_B \int_{t_0}^{t_{end}} (Q^{PORFC}_{cyc,SOC}) dt,$$

$$Q^{PORFC}_{cyc,SOC} = \frac{1}{T_{ctrl}} \sum_{c=1}^{2} Q^{\text{PORFC}}_{cyc,c,SOC} \left(SOC(t), SOC^{\text{PORFC}}_{m,c}(t), SOC^{\text{PORFC}}_{w,c}(t) \right), \quad (14)$$

where the weight factor w_B represents the unit replacement cost of the battery [10].

Finally, the ENMPC optimization problem is subjected to the system dynamics of the hybrid plant, as shown in Eq. (10b), to the inequality constraints on augmented states, as shown in Eq. (10c), to the box constraints on control and slack variables, as shown in Eq. (10d) and (10e), and to the power balance as equality constraint, as shown in Eq. (10f). Here in Eq. (10f), the term $\eta_{gen}\omega T_g$ represents the electrical power output of wind turbine, where η_{gen} is the generator efficiency.

3.4. MHE optimization problem

The MHE formulation described in this section is based on [19]. MHE utilizes the system information from the wind turbine plant over a finite past duration (specified using the MHE horizon length $T_{horizon,est}$) to calculate the initial state estimates $\mathbf{x}_{est}(t_0)$ for the current ENMPC step. The MHE optimization problem aims to minimize the deviation of the current estimated output $\mathbf{y}_{est}$ from the measurement values $\mathbf{y}_{meas}$, the deviation of the current state estimates $\mathbf{x}_{est}$ from the previous state estimates $\mathbf{x}_{est,prev}$ (to ensure smoother estimator output over consecutive MHE steps), and the noise variable $\bar{\nu}$ [20, 21].

The objective function is given as

$$\min_{\bar{\boldsymbol{\nu}}} \int_{t_0 - T_{horizon,est}}^{t_0} (||\mathbf{y}_{est} - \mathbf{y}_{meas}||^2_{\mathbf{W}_{meas}} + ||\mathbf{x}_{est} - \mathbf{x}_{est,prev}||^2_{\mathbf{W}_{prev}} + ||\bar{\boldsymbol{\nu}}||^2_{\mathbf{W}_{\bar{\nu}}}) dt, \quad (15)$$

where $\mathbf{y}_{est} = (\mathbf{x}_{est}, \ddot{d}_{T_{FA,est}})$ and $\mathbf{y}_{meas} = (\mathbf{x}_{meas}, \ddot{d}_{T_{FA,meas}})$. The estimated tower fore-aft acceleration $\ddot{d}_{T_{FA,est}}$ is obtained using the nonlinear output equation shown in (5). The measured tower fore-aft acceleration $\ddot{d}_{T_{FA,meas}}$ is obtained from the real plant as a result of standard sensor measurement. The measured tower-tip velocity and tip-deflection are obtained by numerical integration of tip acceleration and velocity, respectively. The diagonal weighting matrices $\mathbf{W}_{meas}$, $\mathbf{W}_{prev}$, and $\mathbf{W}_{\bar{\nu}}$ are subject to tuning depending on the desired performance from the estimator.

The optimization problem is only subjected to estimator system dynamics

$$\dot{\mathbf{x}}_{est} = \mathbf{F}_{est}(\mathbf{x}_{est}(t), \mathbf{d}_{est}(t)) + \boldsymbol{\nu}(t), \quad (16)$$

where $\mathbf{d}_{est}(t) = (V_w(t), \beta_b(t), \dot{T}_g(t))$ are the disturbance input to the system, which are already set by the ENMPC and are hence fixed for present MHE step. Here, $\mathbf{x}_{est}$ represents the estimator system states which are equivalent to the wind turbine system states $\mathbf{x_{WT}}$ shown in Sect. 3.1. Moreover, $\mathbf{F}_{est}(\cdot)$ represents the system of ordinary differential equations for wind turbine dynamics shown in Sect. 3.1.1.

After the execution of an MHE step, the terminal state at the end of the MHE horizon becomes the initial state at the beginning of the ENMPC prediction horizon $\mathbf{x_{WT}}_0 = \mathbf{x_{WT}}(t_0) = \mathbf{x}_{est}(t_0)$.

4. Simulation setup and results

The formulated economic nonlinear MPC-MHE problem is solved via the state-of-the-art *ACADOS* framework [22], using the interior-point solver *HPIPM* for the underlying Quadratic Programs (QP) in the Nonlinear Program (NLP). A single QP is solved per ENMPC step using the multiple shooting approach with a newton step length of 1, and the Hessian matrix is automatically convexified to address possible numerical issues due to the highly non-standard formulation produced by PORFC [9]. The ENMPC and MHE horizon lengths $T_{horizon}$ and $T_{horizon,est}$ are set to $4s$ each with a total of 20 discretization steps each, such that the sample time T_{ctrl} for both ENMPC and MHE is $200ms$. The wind turbine plant model, based on *OpenFAST* simulator, is sampled every $5ms$. The optimal control inputs applied to the wind turbine plant model are considered as piece-wise constant over T_{ctrl} as $T_{ctrl} > 5ms$. The battery plant model is sampled at T_{ctrl}. The hybrid plant measurements $\widetilde{\mathbf{x}}$ are obtained every T_{ctrl}.

Fig. 1 shows the simulation output for the formulated ENMPC-MHE setup for closed-loop operation of a high-fidelity wind turbine and battery based hybrid generation system. The input wind speed is obtained using DLC 1.2 wind profile and the hybrid plant is subjected to a varying power demand around the rated wind power generation. The formulated ENMPC using PORFC is compared first with a base-case scenario similar to Eq. (10) but with the only difference in the optimization objective which only focuses on maximizing power capture instead of maximizing profit (as in Eq. (10)).

The net profit is calculated as the difference of revenue from wind power generation and costs due to tower fatigue damage and battery capacity loss. The revenue is calculated as a product of revenue rate w_P and wind turbine electrical power output $\eta_{gen}\omega T_g$. Although the formulated ENMPC controller only minimizes tower fatigue due to tower fore-aft stress, the impact of control actions on the tower side-side oscillations are also considered by evaluating the projected cost of tower fatigue. First, the tower fore-aft $\sigma_{FA}(t)$ and side-side oscillations $\sigma_{SS}(t)$, obtained from the plant model, are projected along all the azimuth directions of tower base, then the cost of cyclic fatigue damage for each of these projections is evaluated to finally obtain the maximum of these costs. This way, any possible increase/decrease in tower side-side stress oscillations due to control actions aimed for minimizing tower fore-aft stress is taken into account. The cost of cyclic fatigue damage for each of the projections for a given azimuth direction is obtained by first performing RFC analysis on the projected stress trajectory, then applying Goodman equation for mean stress correction, then obtaining damage cost of each stress cycle by the tower material S-N curve and the component cost, and then applying Miner-Palmgren algorithm to sum up the cost of individual cycles to finally obtain the total cost (refer [23] for detailed formulation). The cost of battery damage is obtained by first performing RFC analysis on $SOC(t)$, then applying Woehler curve mapping to obtain equivalent damage per cycle, then summing up the damage over all the identified cycle, and finally multiplying it with w_B to obtain the total cost (refer [10] for detailed formulation).

The simulation results show that the formulated ENMPC controller (shown as dark green solid line in Fig. 1) performs economically better than the base-case scenario (shown as dark blue solid line in Fig. 1). The enhanced economic performance is due to the fact that the formulated controller manages to find the optimal operational spot, which balances the wind turbine tower fatigue cost and revenue from power generation while utilizing the battery more. The additional cost of battery damage (refer to Fig. 1.h) due to higher utilization (refer to Fig. 1.k) is smaller in magnitude than the reduction in wind turbine fatigue (refer to Fig. 1.g) due to a significant reduction in the tower oscillation amplitudes (refer to Fig. 1.i and to Fig. 1.j). Even though the revenue is slightly lower (refer to Fig. 1.f), the resultant cumulative profit (refer to Fig. 1.e) is higher by 30% compared to the base-case scenario.

Additionally, the formulated ENMPC, which utilizes a direct fatigue penalization approach (refer to Eq. (12)) using PORFC, is compared against a TTVP-based ENMPC which utilizes

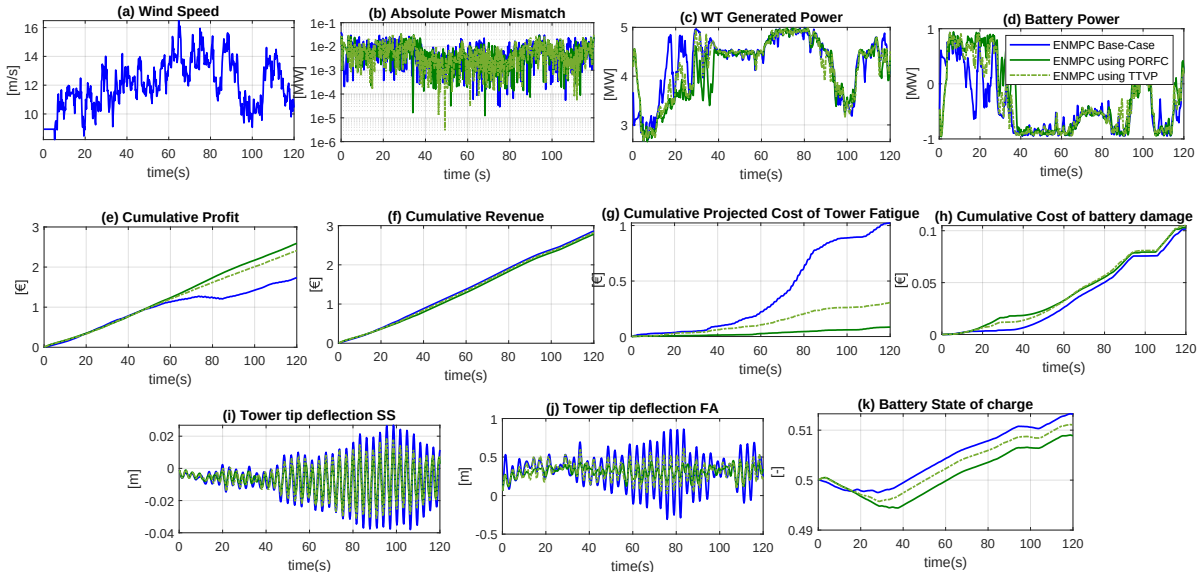

Figure 1: Simulation output for closed-loop economic control of a wind-battery hybrid system

the indirect fatigue penalization approach (refer to Eq. (13)). The tunable weight parameter $w_{fatigue}^{TTVP}$ is obtained by running multiple closed-loop simulations to perform a parameter sweep optimization corresponding to the maximal cumulative profit. The simulation output of ENMPC using TTVP (shown as light green dash-dot line in Fig. 1) also performs economically better than the base-case scenario, highlighting the importance of profit-maximizing operation of a hybrid system instead of power-maximizing operation. Moreover, the importance of accurate fatigue evaluation and direct fatigue penalization can be further seen as the ENMPC PORFC controller performs economically better than the ENMPC TTVP controller (the former results in approximately 7% more cumulative profit than the latter).

Although, for all three closed-loop simulation cases, the absolute power mismatch between total hybrid system generation and demand (refer to Fig. 1.b) is non-zero, the mismatch values are orders of magnitudes smaller than the reference power. Moreover, all three controller formulations satisfy the system state and input constraints. For example, the generated electrical power (refer Fig. 1.c) does not exceed the rated value of 5MW during the above rated wind speed between 60s and 80s.

It should also be highlighted that both the PORFC ENMPC formulation and the TTVP ENMPC formulation manage to reduce amplitudes of tower fore-aft as well as tower side-side oscillations (refer to Fig. 1.j and to Fig. 1.i), even though in both formulations only tower fore-aft fatigue is minimized (refer to Eq. (12) and to Eq. (13)). This shows that both the direct and indirect penalization formulation of the sole tower fore-aft fatigue definitely does not result in increased tower side-side fatigue. In a best case scenario, the fore-aft fatigue minimization objective is in itself sufficient to reduce the tower side-side fatigue damage as well. Moreover, for all the three formulated controllers, tower side-side fatigue cost contributes to less than 5% of the total wind turbine tower fatigue cost. This implies that, even though it is important to take tower side-side fatigue into account while evaluating total tower fatigue, this term does not necessarily have to be an optimization objective for the economic control of the considered wind turbine under the formulated inflow condition. A detailed validation of the impact of side-side fatigue might be needed for a different setup. Furthermore, since the fore-aft objective function has positive impact on side-side fatigue, also a side-side objective function could lead to benefits for fore-aft fatigue, which will be tested in future work.

Moreover, as both ENMPC and MHE are formulated using pre-compiled C code generated by the *ACADOS* framework, both are individually real-time feasible. For the ENMPC and MHE, sample times of 200ms have been set. The maximum computation times during the 120s simulation duration were found to be 185ms and 150ms, respectively. Thus, for instance, by moderate reductions of horizon lengths, also the combination of ENMPC and MHE could be rendered real-time feasible. Strict real-time feasibility, however, has not been the focus of the present work.

5. Conclusion

An ENMPC coupled with an MHE for closed-loop control of a hybrid wind-battery generation system was formulated in this work. The ENMPC aimed to maximize generator profit, in the presence of plant model mismatch, by balancing between revenue accrued due to wind power generation and costs incurred due to wind turbine tower fatigue and battery cyclic fatigue damages, while following a total power generation command. The discontinuous nature of the standard RFC formulation within ENMPC was addressed using the parametric online RFC approach, which externalizes the damage evaluation process from the ENMPC optimization step and also takes into account the impact of stress histories. The MHE provided for the initialization of states for the reduced order internal model of ENMPC, and estimated states that could not be measured directly on a real plant.

The simulation results showed that the formulated parametric online RFC based ENMPC results in significant profit gain against a realistic base-case scenario with suitable dynamic performance, as well as constraint satisfaction. Moreover, the formulated controller also performed economically better than another standard ENMPC. The impact of tower side-side dynamics on overall economic performance was assessed. It was concluded that, although it is important to consider side-side dynamics while evaluating tower fatigue, it does not necessarily have to be an optimization objective. As next steps, the present formulation will be extended to have a more holistic economic objective. This includes not only capturing the fatigue damage of other components, such as blades, drive-train etc., but also having a more realistic profit evaluation model, as the current profit formulation neglects effect of fatigue on O&M expenses and considers only the cost due to tower fatigue. The future work will also include considering a detailed setup of modern electricity grids and energy markets. Another considered extension of this work is to evaluate and validate the impact of side-side fatigue damage under different wind input conditions, particularly in the presence of horizontal wind shear or yaw misalignment.

References

[1] Canet H, Loew S and Bottasso C L 2021 *Wind Energy Science* **6** 1325–1340
[2] Stehly T, Beiter P and Duffy P URL `https://www.osti.gov/biblio/1756710`
[3] Barré A, Deguilhem B, Grolleau S, Gérard M, Suard F and Riu D 2013 *Journal of Power Sources* **241** 680–689 ISSN 03787753
[4] Abdeltawab H H and Mohamed Y A R I 2015 *IEEE Transactions on Industrial Electronics* **62** 6658–6670 ISSN 0278-0046
[5] Rodriguez R H L, Vechiu I, Jupin S, Bacha S, Tabart Q and Pouresmaeil E 2018 A new energy management strategy for a grid connected wind turbine-battery storage power plant *2018 IEEE International Conference on Industrial Technology (ICIT)* pp 873–879
[6] Wang C, Du Z, Ni Y, Li C and Zhang G 2018 *IET Generation, Transmission & Distribution* **12** 2406–2414 ISSN 1751-8687
[7] Anand A, Loew S and Bottasso C L 2021 Economic control of hybrid energy systems composed of wind turbine and battery *2021 European Control Conference (ECC)* pp 2565–2572
[8] ASTM 1985 Standard practices for cycle counting in fatigue analysis
[9] Loew S, Obradovic D and Bottasso C L 2020 *Journal of Physics: Conference Series* **1618** 022041 ISSN 1742-6596
[10] Loew S, Anand A and Szabo A 2021 *Energy Storage* ISSN 2578-4862

[11] Marsh G, Wignall C, Thies P R, Barltrop N, Incecik A, Venugopal V and Johanning L 2016 *International Journal of Fatigue* **82** 757–765 ISSN 01421123
[12] Shi Y, Xu B, Tan Y, Kirschen D and Zhang B 2019 *IEEE Transactions on Automatic Control* **64** 2324–2339 ISSN 0018-9286
[13] Loew S and Obradovic D 2018 Real-time implementation of nonlinear model predictive control for mechatronic systems using a hybrid model *2018 IEEE 14th International Conference on Automation Science and Engineering (CASE)* pp 164–167
[14] Gao Z, Chin C, Woo W and Jia J 2017 *Energies* **10** 85
[15] Jonkman J, Butterfield S, Musial W and Scott G URL `https://www.osti.gov/biblio/947422`
[16] Gros S 2013 An economic nmpc formulation for wind turbine control *52nd IEEE Conference on Decision and Control* pp 1001–1006
[17] Barradas-Berglind J J and Wisniewski R 2016 *Wind Energy* **19** 2189–2203 ISSN 10954244
[18] Gros S and Schild A 2017 *International Journal of Control* **90** 2799–2812 ISSN 0020-7179
[19] Loew S and Bottasso C L 2021 Lidar-assisted model predictive control of wind turbine fatigue via online rainflow-counting considering stress history [preprint] *Wind energy Science (Discussions)*
[20] Gros S, Vukov M and Diehl M 1007–1012
[21] Huang R, Biegler L T and Patwardhan S C 2010 *Industrial & Engineering Chemistry Research* **49** 7882–7890 ISSN 0888-5885
[22] Verschueren R, Frison G, Kouzoupis D, van Duijkeren N, Zanelli A, Quirynen R and Diehl M 2018 Towards a modular software package for embedded optimization *Proceedings of the IFAC Conference on Nonlinear Model Predictive Control (NMPC)*
[23] Loew S, Obradovic D and Bottasso C L 2022 *Optimal Control Applications and Methods*